INTERNATIONAL JOURNAL OF
NUMERICAL ANALYSIS AND MODELING
Volume 16, Number 3, Pages 398–411

CONVERGENCE TO EQUILIBRIUM OF A DC ALGORITHM FOR AN EPITAXIAL GROWTH MODEL

HAMZA KHALFI, MORGAN PIERRE, NOUR EDDINE ALAA, AND MOHAMMED GUEDDA

Abstract. A linear numerical scheme for an epitaxial growth model is analyzed in this work. The considered scheme is already established in the literature using a convexity splitting argument. We show that it can be naturally derived from an optimization viewpoint using a DC (difference of convex functions) programming framework. Moreover, we prove the convergence of the scheme towards equilibrium by means of the Lojasiewicz-Simon inequality. The fully discrete version, based on a Fourier collocation method, is also analyzed. Finally, numerical simulations are carried out to accommodate our analyzis.

Key words. Thin film epitaxy, DC programming, coarsening dynamics, Lojasiewicz-Simon inequality, epitaxial growth, model without slope selection, Fourier spectral method, convergence to equilibrium, pattern formation.

1. Introduction

We are concerned in this paper with the dynamics of the following model of thin film epitaxial growth:

$$\frac{\partial h}{\partial t} = -\nabla \cdot \left(\frac{\nabla h}{1 + |\nabla h|^2} \right) - \delta \Delta^2 h \tag{1}$$

where $h : \Omega \times [0, \infty) \to \mathbb{R}$, is a height function of a thin film in a co-moving frame, $\Omega = (0, L)^d$ for $d = 1, 2$ and δ is a nonnegative constant.

The nonlinear term on the right-hand side, the Ehrlich-Schwoebel barrier defined in [19, 17], is the destabilizing surface which was first proposed phenomenologically in the field of molecular beam epitaxy in [8]. The effect of this last term is counterbalanced by the classical linear Mullin regularising term. This last term describes relaxation through surface diffusion. Even though equation (1) describes a physical process far from equilibrium, it happens to be associated with a gradient flow with respect to the L^2 inner product of the free energy functional:

$$\mathcal{J}(h) = \int_\Omega \frac{1}{2} \left(\delta |\Delta h|^2 - \ln \left(1 + |\nabla h|^2 \right) \right). \tag{2}$$

The energy above is known to behave badly, this was mentioned in many references [3, 11], due to the presence of the negative logarithmic term and in fact it is poorly understood mathematically. This model takes its name from the fact that the energy has no relative minima, which implies that there is no energetically favourable value for $|\nabla h|$. Hence the naming without slope selection model.

Fourth order partial differential equations (PDEs) present in general many theoretical and numerical challenges. In the context of molecular beam epitaxy, the considered model attracted the attention of many researchers. In fact, an analytical approach has been carried out in [4] and later on by Guedda *et al.* in [6] in

Received by the editors November 9, 2017 and, in revised form, September 30, 2018.
2000 *Mathematics Subject Classification.* 35R35, 49J40, 60P40.

order to understand the predicted pyramidal structures characterized by the absence of a preferred slope. The authors show the existence of similarity solutions which predict the typical coarsening process in the limit of larger slope. The results obtained confirm that the typical mound lateral size and the interfacial width grow with time like $t^{\frac{1}{2}}$ and $t^{\frac{1}{4}}$ respectively. In [13], authors studied the free energy in order to understand the interfacial dynamics using energetic arguments and in order to justify rigorously the scaling laws predicted by the model. The authors show that for any $\delta > 0$, $\mathcal{J}$ admits global minimizers h_δ among the class of smooth and periodic height profiles having a null mean value. Li and Liu showed the well posedness and regularity of the solution to the problem (1). Moreover, they prove bounds and error estimates for Galerkin spectral approximation [12].

Numerical investigations of the model without slope selection are extensively studied in the literature. This is due to computational complexity and the long simulation time needed to predict the scaling laws. Moreover, these laws are expected to break down the closer one gets to equilibrium. Many attempt to design linear numerical schemes were made in order to overcome this difficulty. We cite here the reference [3] and the work in [18] where a second-order linearised three-level backward Euler scheme was proposed. Long time simulations for the coarsening process were performed and physically interesting quantities namely the surface roughness, the mound width, saturation time and the energy were computed in order to recover the scaling laws. However this come at the expense of a high computational cost. It could be interesting to focus on second order schemes in the spirit of the recent work [11] where a second order operator splitting Fourier method to tackle the numerical integration of Equation (1). Although linear, such schemes require three step integrations which increase complexity and therefore are neglected at the present time. Cheng and co-authors [1] proposed the first order linear scheme we are considering in this paper. They proved the unconditional stability and solvability of the fully discrete scheme and showed numerical simulations using a collocation-type Fourier spectral differentiation. Related schemes were proposed in [2, 9].

Our aim in this paper is to prove and numerically analyze the convergence to an equilibrium of the time semidiscrete linear scheme established in [1]. Convergence to a single equilibrium is not obvious because there is typically a continuum of critical points for the functional $\mathcal{J}$, due to the periodic boundary conditions. For the continuous-in-time equation (1), it has been proved by Grasselli *et al.* [5] by means of a Lojasiewicz-Simon inequality. Our proof is similar to the approach in [15, 16], but the novelty is that the scheme here is *linearly* implicit and not fully implicit. We will also consider the fully discrete scheme, where the space discretization is the Fourier spectral collocation method from [1].

The layout of the paper is organized as follows: we start our manuscript by stating the problem and recovering the expression of the linear scheme using a DC programming framework (Section 2). In Section 3, we show the convergence of the algorithm towards a critical value of the functional (2) by using a Lojasiewicz-Simon inequality. We prove a similar result for the fully discrete scheme in Section 4. Numerical simulations accommodated with some interpretations are presented in Section 5. Finally, a summary and conclusion are drawn in the last section.

2. Formulation of the DC algorithm

In the same framework as [13], we analyze the problem of minimizing $\mathcal{J}$ over the class of smooth periodic height function:

$$\mathcal{H}(\Omega) = \left\{ u \in H^2_{per}(\Omega) \,/\, \int_\Omega u \, \mathrm{dx} = 0 \right\}. \tag{3}$$

Throughout the paper, and for an integer k, $H^k_{per}(\Omega)$ denotes the usual Sobolev space of functions which are L-periodic in the d-dimensions ($d = 1, 2$). It is a Hilbert space based on the $L^2(\Omega)$ space. The topological dual of $H^k_{per}(\Omega)$ is denoted $[H^k_{per}(\Omega)]'$.

In the remainder of the paper we set $A \geq 1/8$. We recall that $\delta > 0$. We define

$$H(h) = \frac{1}{2}\int_\Omega \left(\delta \, |\Delta h|^2 + A \, |\nabla h|^2 \right) \, \mathrm{dx}, \tag{4}$$

$$G(h) = \frac{1}{2}\int_\Omega \left(A \, |\nabla h|^2 + \ln\left(1 + |\nabla h|^2\right) \right) \, \mathrm{dx}. \tag{5}$$

Even if $\mathcal{J}$ is not convex, it can be written as a difference of two convex functions in $H^2_{per}(\Omega)$. Namely, $\mathcal{J} = H - G$, where the functions H and G are convex and nonnegative. Indeed, it has been proved in [9, Proposition 2.1] that for $A \geq 1/8$, the function $g : \mathbb{R}^2 \to \mathbb{R}$ defined by

$$g(v_1, v_2) = A(v_1^2 + v_2^2) + \ln\left(1 + v_1^2 + v_2^2\right)$$

is convex, and that the value $A = 1/8$ is optimal. This implies that G is also convex. The couple (H, G) is called a DC decomposition of $\mathcal{J}$.

We note that H and G are continuously differentiable on $H^2_{per}(\Omega)$ and that $h \in H^2_{per}(\Omega)$ is a critical point of $\mathcal{J}$ if

$$\mathcal{J}'(h) := \delta \Delta^2 h + \mathrm{div}\left(\frac{\nabla h}{1 + |\nabla h|^2} \right) = 0$$

in $[H^2_{per}(\Omega)]'$.

In the same spirit as [20], the DC algorithm can be stated as follows:

$$\begin{cases} h_0 \in \mathcal{H}(\Omega), \\ \dfrac{h_{n+1}}{\lambda} - A\Delta h_{n+1} + \delta \Delta^2 h_{n+1} = \dfrac{h_n}{\lambda} - A\Delta h_n - \mathrm{div}\left(\dfrac{\nabla h_n}{1 + |\nabla h_n|^2} \right). \end{cases} \tag{6}$$

Here, λ is a positive parameter which can be interpreted as an artificial time step. The scheme above enforces the use of explicit time discretisation for the nonlinearity while handling the linear terms implicitly. In addition, the originally ill-posed problem is regularised by the additional laplacian term. It is obvious that the scheme is linear and well posed. The existence and uniqueness of h_{n+1} are actually guaranteed because the operator $(\frac{1}{\lambda} I - A\,\Delta + \delta\,\Delta^2)$ is invertible from $H^2_{per}(\Omega)$ into $[H^2_{per}(\Omega)]'$, due to the standard Lax-Milgram theory. Since $h_0 \in \mathcal{H}(\Omega)$, we have $h_n \in \mathcal{H}(\Omega)$ for every n.

3. Convergence to equilibrium for the linear DC algorithm

We first note that the functional space $\mathcal{H}(\Omega)$ defined by (3) has the following properties: the map $u \mapsto ||\Delta u||_{L^2}$ is a norm on $\mathcal{H}(\Omega)$ which is equivalent to the

$H^2_{per}(\Omega)$-norm, and for all $h \in \mathcal{H}(\Omega)$,

$$||h||_{L^2} \leq c_1||\nabla h||_{L^2}, \tag{7}$$

$$||\nabla h||_{L^2} \leq c_2||\Delta h||_{L^2}. \tag{8}$$

The following result, which is proved in [13, Lemma 4.2], shows that the energy is bounded from below.

Proposition 1. *Let $\delta > 0$ and $\nu = \dfrac{\delta}{2\ c_2^2}$. Then there exist $s_\nu \geq 0$ such that*

$$\mathcal{J}(h) \geq -\frac{|\Omega|}{2}\ln(1+s_\nu) + \frac{\delta}{4}\int_\Omega |\Delta h|^2, \quad \forall h \in \mathcal{H}(\Omega). \tag{9}$$

As in [1, 9], we prove that the convex splitting guarantees the stability of the scheme.

Theorem 2. *The sequence $(\mathcal{J}(h_n))_n$ is nonincreasing. Moreover, there exist a critical point h of $\mathcal{J}$ and a subsequence of $(h_n)_n$ converging to h weakly in $H^2_{per}(\Omega)$.*

Proof. The DC Algorithm (6) reads

$$\frac{1}{\lambda}(h_{n+1}-h_n) - A\ \Delta h_{n+1} + \delta\Delta^2 h_{n+1} = -A\ \Delta h_n - \nabla\cdot\left(\frac{\nabla h_n}{1+|\nabla h_n|^2}\right). \tag{10}$$

On multiplying by $(h_{n+1}-h_n)$, integrating on Ω and using the identity $a\cdot(a-b) = \frac{1}{2}\left(a^2-b^2+(a-b)^2\right)$, we obtain

$$\begin{aligned}
&\frac{1}{\lambda}\int_\Omega |h_{n+1}-h_n|^2 + \frac{A}{2}\int_\Omega |\nabla h_{n+1}|^2 - \frac{A}{2}\int_\Omega |\nabla h_n|^2 + \frac{A}{2}\int_\Omega |\nabla h_{n+1}-\nabla h_n|^2\\
&+\frac{\delta}{2}\int_\Omega |\Delta h_{n+1}|^2 - \frac{\delta}{2}\int_\Omega |\Delta h_n|^2 + \frac{\delta}{2}\int_\Omega |\Delta h_{n+1}-\Delta h_n|^2\\
&= \int_\Omega A\nabla h_n\cdot\nabla(h_{n+1}-h_n) + \frac{\nabla h_n\cdot\nabla(h_{n+1}-h_n)}{1+|\nabla h_n|^2}.
\end{aligned} \tag{11}$$

Since G (see (5)) is convex and differentiable on $H^2_{per}(\Omega)$, standard calculus shows that (see e.g. [10])

$$G(h) - G(\bar h) \geq \langle G'(\bar h), h-\bar h\rangle := \int_\Omega A\nabla\bar h\cdot\nabla(h-\bar h) + \frac{\nabla\bar h\cdot\nabla(h-\bar h)}{1+\left|\nabla\bar h\right|^2},$$

for all $h, \bar h \in H^2_{per}(\Omega)$. On choosing $\bar h = h_n$, $h = h_{n+1}$ and plugging this into (11), we find (recall (4))

$$\begin{aligned}
&\frac{1}{\lambda}\int_\Omega |h_{n+1}-h_n|^2 + \frac{A}{2}\int_\Omega |\nabla h_{n+1}-\nabla h_n|^2 + \frac{\delta}{2}\int_\Omega |\Delta h_{n+1}-\Delta h_n|^2\\
&+H(h_{n+1}) - H(h_n) \leq G(h_{n+1}) - G(h_n),
\end{aligned}$$

that is

$$\begin{aligned}
&\frac{1}{\lambda}\int_\Omega |h_{n+1}-h_n|^2 + \frac{A}{2}\int_\Omega |\nabla h_{n+1}-\nabla h_n|^2 + \frac{\delta}{2}\int_\Omega |\Delta h_{n+1}-\Delta h_n|^2\\
&\leq \mathcal{J}(h_n) - \mathcal{J}(h_{n+1}).
\end{aligned} \tag{12}$$

Therefore, the sequence $(\mathcal{J}(h_n))_n$ is nonincreasing and bounded from below, so it converges to some real number α. Since, by (9),

$$\frac{\delta}{4}\int_\Omega |\Delta h_n|^2 \leq \mathcal{J}(h_1) + \frac{|\Omega|}{4}\ln(1+s_\nu),$$

there exists a subsequence $(h_{n_k})_k$ and h such that

$$h_{n_k} \rightharpoonup h \qquad \text{in } H^2_{per}(\Omega). \tag{13}$$

It remains to see that h is a critical point. By adding terms in (12), and tending to a limit, we obtain

$$c \sum_{n=1}^{\infty} \int_\Omega |h_{n+1} - h_n|^2 + |\nabla h_{n+1} - \nabla h_n|^2 + |\Delta h_{n+1} - \Delta h_n|^2 \leq \mathcal{J}(h_1) - \alpha. \tag{14}$$

where $c = \min(\frac{1}{\lambda}, \frac{A}{2}, \frac{\delta}{2})$. In particular,

$$\|h_{n+1} - h_n\|^2_{H^2} \to 0, \tag{15}$$

and the left-hand side of (10) converges in $[H^2_{per}(\Omega)]'$ to $-A\Delta h + \delta\Delta^2 h$ (up to the subsequence $(h_{n_k})_k$). Finally, we note that the sequence

$$\frac{\nabla h_n}{1 + |\nabla h_n|^2}$$

is bounded in $L^\infty(\Omega)$, so that, up to a subsequence, we have

$$\frac{\nabla h_n}{1 + |\nabla h_n|^2} \to \frac{\nabla h}{1 + |\nabla h|^2},$$

weakly in $L^2(\Omega)$ and a.e. in Ω. Thus, the right-hand side of (10) converges (up to a subsequence) to

$$-A\Delta h - \nabla \cdot \left(\frac{\nabla h}{1 + |\nabla h|^2} \right),$$

which is therefore equal to $-A\Delta h + \delta\Delta^2 h$. This shows that h is indeed a critical point of $\mathcal{J}$. □

We note that (14) is not sufficient to establish the convergence of the whole sequence. Our purpose is to prove this result using the Lojasiewicz-Simon inequality (Lemma 4).

In the following, we define the ω-limit set of the sequence $(h_n)_n$ by

$$\omega((h_n)_n) = \{h \in H^3_{per}(\Omega) \cap \mathcal{H}(\Omega),\ \exists n_k \longrightarrow \infty,\ h_{n_k} \longrightarrow h \text{ strongly in } H^3_{per}(\Omega)\}. \tag{16}$$

We have:

Proposition 3. *The set $\omega((h_n)_n)$ is a compact and connected subset of $H^3_{per}(\Omega)$.*

Proof. We already know that the sequence (h_n) is bounded in $H^2_{per}(\Omega)$. We will show that the right-hand side of the DC algorithm (6) is bounded in $L^2(\Omega)$. By elliptic regularity, this will imply that the sequence $(h_{n+1})_n$ is bounded in $H^4_{per}(\Omega)$. Now, the first terms (h_n) and (Δh_n) in (6) are obviously bounded in $L^2(\Omega)$. We only need to control the nonlinearity, which can be written as

$$\text{div}\left(\frac{\nabla h_n}{1 + |\nabla h_n|^2} \right) = \frac{\Delta h_n}{1 + |\nabla h_n|^2} - \frac{2}{\left(1 + |\nabla h_n|^2\right)^2} \left(D_2(h_n)\ \nabla h_n\right) \cdot \nabla h_n, \tag{17}$$

where $D_2(h_n) = (\partial_{x_i x_j} h_n)_{1 \leq i,j \leq d}$ is the hessian matrix of h_n. In the right-hand side above, the term $\frac{\Delta h_n}{1+|\nabla h_n|^2}$ is bounded in $L^2(\Omega)$, since $\frac{1}{1+|\nabla h_n|^2}$ is bounded (by

1) in $L^\infty(\Omega)$ and Δh_n is bounded in $L^2(\Omega)$. Moreover, by the Cauchy-Schwarz inequality in $\mathbb{R}^d$, the last term above satisfies the pointwise estimate

$$\frac{2}{\left(1+|\nabla h_n|^2\right)^2}\,|(D_2(h_n)\ \nabla h_n)\cdot\nabla h_n| \le \frac{2|\nabla h_n|^2}{1+|\nabla h_n|^2}\|D_2(h_n)\| \le 2\|D_2(h_n)\|,$$

where $\|D_2(h_n)\|$ is the norm of the matrix $D_2(h_n)$ relatively to the Euclidean norm on $\mathbb{R}^d$. Since $D_2(h_n)$ is bounded in $(L^2(\Omega))^{d^2}$, this shows that the right-hand side of (17) is bounded in $(L^2(\Omega))$, as claimed. Thus, (h_n) is bounded in $H^4_{per}(\Omega)$ and therefore the ω-limit set is compact in $H^3_{per}(\Omega)$.

Using (15), this compactness in $H^3_{per}(\Omega)$ implies that $\|h_{n+1}-h_n\|_{H^3}\to 0$. Then, a standard contradiction argument shows that the set $\omega((h_n)_n)$ is also connected in $H^3_{per}(\Omega)$. □

In [5], Grasselli and his collaborators obtained a suitable Lojasiewicz-Simon inequality for the model without slope selection (1) in the case of Neumann boundary conditions. Their inequality still holds in the case of periodic boundary conditions. The proof is similar and even easier since the boundary is much more regular here (see also the recent review [7]). Our proof of the main result is based on their inequality adapted to our setting. It reads:

Lemma 4. *Let $h^\star \in H^3_{per}(\Omega)\cap\mathcal{H}(\Omega)$ be a critical point of the energy functional $\mathcal{J}$. Then there exist $\theta\in]0,\frac{1}{2}[$ and $\sigma>0$ (which depend on $h^\star$) such that for all $h\in H^3_{per}(\Omega)\cap\mathcal{H}(\Omega)$,*

$$\|h-h^\star\|_{H^3}<\sigma \Longrightarrow |\mathcal{J}(h)-\mathcal{J}(h^\star)|^{1-\theta}\le \|\mathcal{J}'(h)\|_{(H^3_{per})'}. \tag{18}$$

We are now in position to prove:

Theorem 5. *The whole sequence $(h_n)_n$ converges to a critical point h of $\mathcal{J}$ in $H^3_{per}(\Omega)$.*

Proof. The proof of Theorem 2 shows that every $h\in\omega((h_n)_n)$ is a critical point of $\mathcal{J}$. Moreover, $\mathcal{J}(h_n)$ is nonincreasing and tends to α, so that $\mathcal{J}$ is equal to α on $\omega((h_n)_n)$.

If $\mathcal{J}(h_{n_0})=\alpha$ for some n_0, then $\mathcal{J}(h_n)=\alpha$ for $n\ge n_0$, and by (12), the sequence $(h_n)_{n\ge n_0}$ is constant, and the result is obvious. Thus, we may assume that $\mathcal{J}(h_n)>\alpha$ for all n, and we will set $\tilde{\mathcal{J}}(h)=\mathcal{J}(h)-\alpha$. By (12), we have

$$\tilde{\mathcal{J}}(h_n)-\tilde{\mathcal{J}}(h_{n+1})=\mathcal{J}(h_n)-\mathcal{J}(h_{n+1})\ge c\|h_{n+1}-h_n\|^2_{H^2}, \tag{19}$$

for some generic constant $c>0$.

For every $h^\star\in\omega((h_n)_n)$, there exist $\theta\in]0,1/2[$ and $\sigma>0$ which may depend on $h^\star$ such that the inequality (18) holds for every $h\in B_\sigma(h^\star)$, where

$$B_\sigma(h^\star):=\{h\in H^3_{per}(\Omega)\cap\mathcal{H}(\Omega),\ \|h-h^\star\|_{H^3}<\sigma\}.$$

The union of balls $\{B_\sigma(h^\star)\ :\ h^\star\in\omega((h_n)_n)\}$ forms an open covering of $\omega((h_n)_n)$. Due to the compactness of $\omega((h_n)_n)$ in $H^3_{per}(\Omega)$, we can find a finite subcovering $\{B_{\sigma_i}(h_i^\star)\}_{i=1,\dots,m}$ such that the constants θ_i and σ_i in (18) are indexed by i. From the definition of $\omega((h_n)_n)$, we know that there exists n_0 large enough such that $h_n\in\mathcal{U}:=\cup_{i=1}^m B_{\sigma_i}(h_i^\star)$ for $n\ge n_0$. Taking $\theta=\min_{i=1}^m\{\theta_i\}$, we deduce from (18) that for all $n\ge n_0$,

$$[\mathcal{J}(h_n)-\alpha]^{1-\theta}\le\|\mathcal{J}'(h_n)\|_{(H^3_{per})'}. \tag{20}$$

On one hand, we have

$$\begin{aligned}
[\tilde{\mathcal{J}}(h_n)]^\theta - [\tilde{\mathcal{J}}(h_{n+1})]^\theta &\geq \theta[\tilde{\mathcal{J}}(h_n)]^{\theta-1} \quad [\tilde{\mathcal{J}}(h_n) - \tilde{\mathcal{J}}(h_{n+1})] \\
&\overset{(19)}{\geq} c\ \theta[\tilde{\mathcal{J}}(h_n)]^{\theta-1} \quad \|h_{n+1} - h_n\|_{H^2}^2 \\
&\geq c\ \theta[\tilde{\mathcal{J}}(h_n)]^{\theta-1} \quad \|h_{n+1} - h_n\|_{H^2}\|h_{n+1} - h_n\|_{H^1}, \qquad (21)
\end{aligned}$$

where here and in the following, c denotes a generic constant independent of n. On the other hand,

$$\begin{aligned}
\mathcal{J}'(h_n) &= \operatorname{div}\left(\frac{\nabla h_n}{1+|\nabla h_n|^2}\right) + \delta\ \Delta^2 h_n \\
&= -\frac{h_{n+1}-h_n}{\lambda} + A\ \Delta\,(h_{n+1}-h_n) - \delta\Delta^2\,(h_{n+1}-h_n)\,.
\end{aligned}$$

Taking the dual norm of $H^3_{per}(\Omega)$ in the expression above, we obtain

$$\|\mathcal{J}'(h_n)\|_{(H^3_{per})'} \leq c\|h_{n+1} - h_n\|_{H^1}.$$

We used here that the dual norm $(H^3_{per})'$ is equivalent to the H^{-3}_{per}-norm which can be defined by means of a spectral decomposition of the operator $-\Delta$ on $H^2_{per}(\Omega)$. By substitution in the inequality (21) and by using the (global) Lojasiewicz inequality (20), we find

$$[\tilde{\mathcal{J}}(h_n)]^\theta - [\tilde{\mathcal{J}}(h_{n+1})]^\theta \quad \geq \quad c\ \|h_{n+1} - h_n\|_{H^2}.$$

From this last inequality, we deduce that the infinite sum $\sum_{n=n_0}^{\infty}\|h_{n+1} - h_n\|_{H^2}$ converges. Thus $(h_n)_n$ is a Cauchy sequence in $H^2_{per}(\Omega)$, therefore it is convergent and by compactness it converges in $H^3_{per}(\Omega)$ as well. □

4. Convergence to equilibrium for the fully discrete linear scheme

For the space discretization, we use a Fourier collocation method, which is known to preserve the convex splitting [1, 9]. We consider the two dimensional case $d = 2$ (the case $d = 1$ is similar). We use a uniform mesh size $h = h_x = h_y = L/N$ where the positive integer $N = N_x = N_y$ is given. All the variables are evaluated at the regular numerical grid (x_i, y_j) with $x_i = ih$, $y_j = jh$, $1 \leq i, j \leq N$.

For a vector $f = (f_{ij},)_{1\leq i,j\leq N}$ over the grid, its discrete Fourier expansion is given by

$$f_{i,j} = \sum_{k,l=-N/2+1}^{N/2} \hat{f}_{k,l} \exp\left(\frac{2k\pi i x_i}{L}\right)\exp\left(\frac{2l\pi i y_j}{L}\right),$$

where the Fourier coefficients are given by

$$\hat{f}_{k,l} = \frac{1}{N^2}\sum_{1\leq i,j\leq N} f_{i,j}\exp\left(-\frac{2k\pi i x_i}{L}\right)\exp\left(-\frac{2l\pi i y_j}{L}\right).$$

Then the Fourier spectral approximations to the first and second order partial derivatives are given by

$$\begin{aligned}
(\mathcal{D}_{N_x} f)_{i,j} &= \sum_{k,l=-N/2+1}^{N/2} \left(\frac{2k\pi i}{L}\right) \hat{f}_{k,l} \exp\left(\frac{2k\pi i x_i}{L}\right) \exp\left(\frac{2l\pi i y_j}{L}\right), \\
(\mathcal{D}_{N_y} f)_{i,j} &= \sum_{k,l=-N/2+1}^{N/2} \left(\frac{2l\pi i}{L}\right) \hat{f}_{k,l} \exp\left(\frac{2k\pi i x_i}{L}\right) \exp\left(\frac{2l\pi i y_j}{L}\right), \\
(\mathcal{D}^2_{N_x} f)_{i,j} &= \sum_{k,l=-N/2+1}^{N/2} \left(-\frac{4\pi^2 k^2}{L^2}\right) \hat{f}_{k,l} \exp\left(\frac{2k\pi i x_i}{L}\right) \exp\left(\frac{2l\pi i y_j}{L}\right), \\
(\mathcal{D}^2_{N_y} f)_{i,j} &= \sum_{k,l=-N/2+1}^{N/2} \left(-\frac{4\pi^2 l^2}{L^2}\right) \hat{f}_{k,l} \exp\left(\frac{2k\pi i x_i}{L}\right) \exp\left(\frac{2l\pi i y_j}{L}\right).
\end{aligned}$$

The discrete Laplacian, gradient and divergence operators become

$$\Delta_N f = \mathcal{D}^2_{N_x} f + \mathcal{D}^2_{N_y} f, \quad \nabla_N f = \begin{pmatrix} \mathcal{D}_{N_x} f \\ \mathcal{D}_{N_y} f \end{pmatrix}, \quad \nabla_N \cdot \begin{pmatrix} f_1 \\ f_2 \end{pmatrix} = \mathcal{D}_{N_x} f_1 + \mathcal{D}_{N_y} f_2,$$

at the pointwise level.

The fully discrete linear DC algorithm reads: let $h^0 = (h^0_{i,j})_{1\le i,j\le N} \in \mathbb{R}^{N^2}$ be defined on the $2d$-grid and for $n = 0, 1, \dots$ let $h^{n+1} \in \mathbb{R}^{N^2}$ solve

$$\frac{h^{n+1}}{\lambda} - A\Delta_N h^{n+1} + \delta \Delta_N^2 h^{n+1} = \frac{h^n}{\lambda} - A\Delta_N h^n - \nabla_N \cdot \left(\frac{\nabla_N h^n}{1 + |\nabla_N h^n|^2}\right), \tag{22}$$

where, as previously, λ and δ are positive constants, and $A \ge 1/8$. This scheme is unconditionally uniquely solvable, because the linear operator involving h^{n+1} is invertible [1]. We note that the gradient is computed in the Fourier space, and the division $\nabla_N h^n$ by $1 + |\nabla_N h^n|^2$ is performed pointwise in the physical space (see Section 5).

Given any grid functions f and g, the discrete approximations to the L^2 norm and inner product are given as

$$\|f\|_2 = \sqrt{\langle f, f\rangle}, \quad \text{with} \quad \langle f, g\rangle = h^2 \sum_{i=1}^{N} \sum_{j=1}^{N} f_{i,j} g_{i,j}.$$

Detailed calculations show that the following discrete integration by parts formulae are valid:

$$\left\langle f, \nabla_N \cdot \begin{pmatrix} g_1 \\ g_2 \end{pmatrix} \right\rangle = -\left\langle \nabla_N f, \begin{pmatrix} g_1 \\ g_2 \end{pmatrix} \right\rangle,$$

and

$$\langle f, \Delta_N g\rangle = -\langle \nabla_N f, \nabla_N g\rangle, \qquad \langle f, \Delta_N^2 g\rangle = \langle \Delta_N f, \Delta_N g\rangle.$$

We define the fully discrete energy via

$$\mathcal{J}_N(h) = \frac{\delta}{2}\|\Delta_N h\|_2^2 - \frac{h^2}{2} \sum_{i=1}^{N} \sum_{j=1}^{N} \ln\left(1 + |\nabla_N h|^2_{i,j}\right), \tag{23}$$

for every vector $h = (h_{i,j})_{1\le i,j\le N}$ defined on the numerical grid.

On defining the convex functions

$$\begin{aligned} H_N(h) &= \frac{\delta}{2}\|\Delta_N h\|_2^2 + \frac{A}{2}\|\nabla_N h\|_2^2, \\ G_N(h) &= \frac{A}{2}\|\nabla_N h\|_2^2 + \frac{h^2}{2}\sum_{i=1}^{N}\sum_{j=1}^{N}\ln\left(1+|\nabla_N h|_{i,j}^2\right), \end{aligned}$$

we see that $\mathcal{J}_N(h) = H_N(h) - G_N(h)$, so that (H_N, G_N) is a DC decomposition of $\mathcal{J}_N$. A vector $h = (h_{i,j})_{1\le i,j\le N}$ is a critical point of $\mathcal{J}_N$ if

$$\mathcal{J}_N'(h) := \Delta_N^2 h + \nabla_N \cdot \left(\frac{\nabla_N h}{1+|\nabla_N h|^2}\right) = 0.$$

On taking the scalar product of (22) by 1, we see that $\langle h^{n+1}, 1\rangle = \langle h^n, 1\rangle$. By induction, $\langle h^n, 1\rangle = \langle h^0, 1\rangle$ for all $n \ge 0$. By analogy with the continuous case, we can work on the $N^2 - 1$ dimensional space

$$\dot{\mathbb{R}}^{N^2} := \{h \in \mathbb{R}^{N^2} \ : \ \langle h, 1\rangle = 0\} = \{h \in \mathbb{R}^{N^2} \ : \ \hat{h}_{0,0} = 0\}.$$

By arguing as in the continuous case, we can show that starting with $h^0 \in \dot{\mathbb{R}}^{N^2}$, the whole sequence (h^n) defined by the fully discrete linear DC algorithm (22) converges to a single equilibrium $h^\star$ in $\mathbb{R}^{N^2}$, where $h^\star$ is a critical point of $\mathcal{J}_N$. The computations are similar, thanks to the analogy between the fully discrete scheme (22) and the time semidiscrete version (6).

The proof is easier, because all norms are equivalent in finite dimension. In particular, since $\|\nabla_N \cdot\|_2$ and $\|\Delta_N \cdot\|_2$ are norms on $\dot{\mathbb{R}}^{N^2}$, they are equivalent to the discrete L^2 norm $\|\cdot\|_2$. Moreover, the Lojasiewicz-Simon inequality (Lemma 4) is replaced by the Lojasiewicz inequality for real analytic functions [14], which reads:

Lemma 6. *Let $h^\star \in \mathbb{R}^{N^2}$ be a critical point of the discrete energy $\mathcal{J}_N$. Then there exist $\theta \in]0, 1/2[$ and $\sigma > 0$ such that for all $h \in \mathbb{R}^{N^2}$,*

$$\|h - h^\star\|_2 < \sigma \Longrightarrow |\mathcal{J}_N(h) - \mathcal{J}_N(h^\star)|^{1-\theta} \le \|\mathcal{J}_N'(h)\|_2.$$

Proof. For every (i,j), the function $h \mapsto \ln(1+|\nabla_N h|_{i,j}^2)$ is real analytic on $\mathbb{R}^{N^2}$ by composition of the quadratic function $h \mapsto |\nabla_N h|_{i,j}^2$ and of the function $v \mapsto \ln(1+v)$ which is real analytic on $(-1, +\infty)$. The function $\mathcal{J}_N$ defined by (23) is a finite sum of such terms and of the quadratic function $h \mapsto (\delta/2)\|\Delta_N h\|_2^2$. Therefore, it is real analytic on $\mathbb{R}^{N^2}$ and the classical Lojasiewicz inequality is valid [7, 14]. □

5. Numerical results and simulations

To simulate the growth dynamics numerically, we proceed as follows for the Fourier spectral algorithm (22).

- **Step 1:** we rewrite the algorithm as:

$$\frac{h^{n+1}}{\lambda} - A\Delta_N h^{n+1} + \delta\Delta_N^2 h^{n+1} = \frac{h^n}{\lambda} - (A+1)\Delta_N h^n + K_N(\nabla_N h^n) \tag{24}$$

where $K_N(\nabla_N h) = \nabla_N \cdot \left(\dfrac{|\nabla_N h|^2}{1+|\nabla_N h|^2}\nabla_N h\right)$.

- **Step 2:** we perform Fourier transform to get:

$$\left(1 + A\lambda\ |k|^2 + \delta\lambda|k|^4\right) \hat{h}_k^{n+1} = \left(1 + (A+1)\lambda\ |k|^2\right) \hat{h}_k^n + \lambda\ (\hat{K}_N)_k \tag{25}$$

  for all $|k| \leq N/2$, where $\hat{h}_k^{n+1}$ and $(\hat{K}_N)_k$ are the Fourier modes of the solution h^{n+1} and the nonlinear term $K_N(\nabla_N h^n)$, respectively (we consider here the 1D case for simplicity). The fixed integer N represents the number of modes. We approximate the nonlinearity using a pseudo-spectral method where we compute the products in the physical space and the resolution in Fourier space.
- **Step 3:** we solve the problem by computing an inverse Fourier transform in order to obtain the desired numerical solution at different times. The parameter λ is taken as an artificial time step.

Using this numerical scheme, we resolve the problem for different scales of the parameters δ in 1D and 2D. We are also interested in the variations of the energy and the roughness of the height profile which is defined by

$$W_n = \sqrt{\frac{1}{|\Omega|} \int_\Omega \left|h^n - \bar{h}^n\right|^2 dx} \tag{26}$$

where $\bar{h}^n$ denotes the mean value of h^n. The quantity W_n is the standard deviation from the mean profile.

5.1. 1D growth dynamics. Here we demonstrate the convergence of the proposed algorithm numerically towards the steady state solution also found in [11] and [12]. We take $\Omega = [0, 12]$, $\delta = 0.25$, $\lambda = 0.005$, $A = 1$, $N = 256$ and we consider the initial condition

$$h_0(x) = 0.1 \left(\sin \frac{2\pi x}{3} + \sin \pi x + \sin \frac{4\pi x}{3} \right). \tag{27}$$

Solutions of the model without slope selection are represented in Figure 1 at different times. In particular, the initial rough-smooth-rough pattern is the same as predicted in [12]. The illustration shows that the initial configuration undergoes different patterns in a direction minimizing the energy which becomes negative after the start of the coarsening of patterns. The results in Figures 1 and 2 were obtained after long time computation. The stopping criteria was taken as $\|h^{n+1} - h^n\| \leq 10^{-15}$. Results are in good agreement with those in [11] and [12].

5.2. 2D growth dynamics. For the case of 2D simulations, we present in Figure 4 the results obtained with $\Omega = [0, 2\pi] \times [0, 2\pi]$, $\delta = 0.001$, $\lambda = 0.1$, $A = 0.5$, $N = 256$ and we consider the initial condition:

$$h_0(x, y) = 0.1 \left(\sin(3x)\sin(2y) + \sin(5x)\sin(5y)\right). \tag{28}$$

The isovalues of the solution h^n is represented at different times. In particular, the initial rough-smooth-rough pattern is more apparent in 2D as in 1D. The illustrations show that the initial configuration consists of two modes, namely mode 3,2 and mode 5,5. The mode 5,5 disappears first, then the vanishing of the other mode leads to the appearance of a new mode.

At time 82, we can see a quasi-steady state, which was reported to be the final steady state in [11] and [12]. In our computation, we pushed all simulation up to a precision of 10^{-15}, we obtained a new final steady state which is identified by a difference $\|h^{n+1} - h^n\|$ of order 10^{-15}. It consists of only one mode which is a critical point of the energy and corresponds to a minimum height profile. A similar

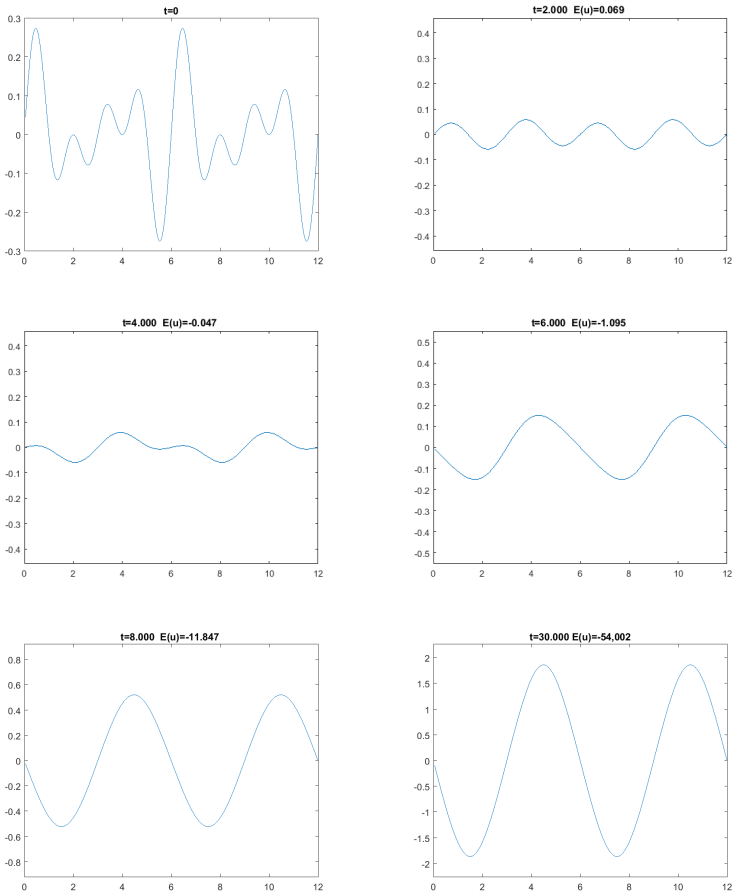

FIGURE 1. Evolution of a 1D height profile starting from an initial configuration (top left) for $\delta = 0.25$.

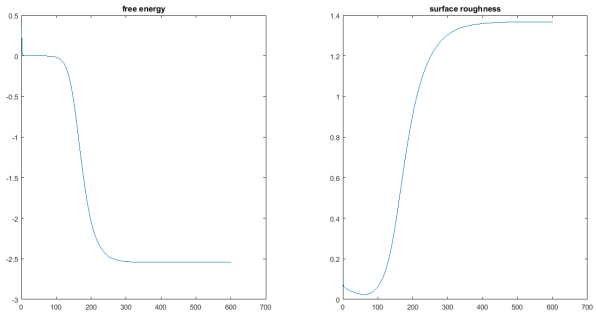

FIGURE 2. 1D Evolution of the energy (left) and roughness (right) for the model without slope selection.

steady state was obtained after a long time computation starting from a random initial condition in [1].

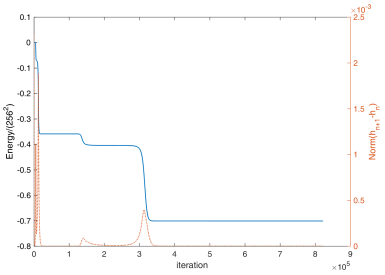

FIGURE 3. 2D Evolution of the energy (left) and the infinity norm of $h_{n+1}-h_n$ (right) for the model without slope selection for $\delta = 0.1$ and $\lambda = 0.001$.

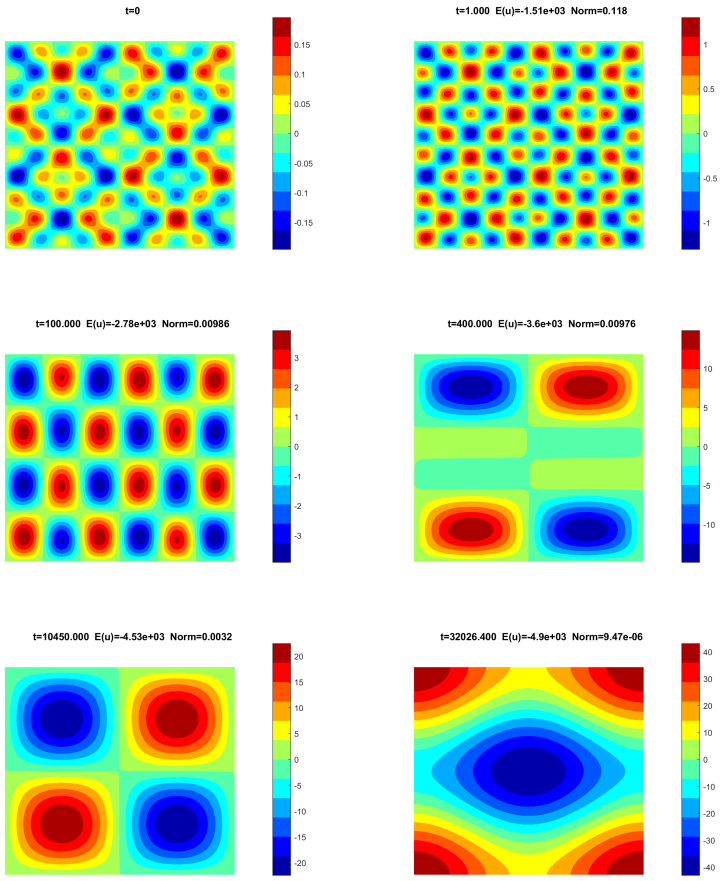

FIGURE 4. 2D Evolution of a height profile starting from an initial configuration given by (28) (top left) for $\delta = 0.001$ and $\lambda = 0.1$.

In Figure 3, we have used the initial value h_0 (28) on $\Omega = [0, 2\pi] \times [0, 2\pi]$, and the parameters are $\delta = 0.1$, $\lambda = 0.001$, $A = 1$ and $N = 256$. The energy, which is represented versus time iterations, has various flat regions, due to coarsening

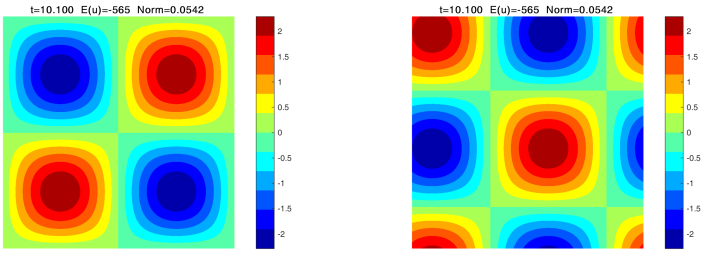

FIGURE 5. Solutions at the time $t = 10.1$ starting from two shifted initial conditions, the first is for (28) and the other for (29).

dynamics. We show the evolution of the norm of the difference $\|h^{n+1} - h^n\|$ in the same plot but with a different scale. We clearly notice that each time the energy has a flat region, the norm of the difference increases and modes fuse in order to reach a further minimum until a precision of 10^{-15} is reached.

We finally consider the shifted initial condition

$$h_0(x, y) = 0.1\,(\sin(3(x+1))\sin(2(y+2)) + \sin(5(x+1))\sin(5(y+2)))\,. \tag{29}$$

with the same parameters as in Figure 3. The dynamics is the same as for the initial value (28), it is only shifted by the same translation through the vector $(-1, -2)$ in Ω, for all times. This is shown in Figure 5, where both solutions are represented at the same time. This illustrates that the energy has a continuum of steady states, by translation invariance. The specific steady state which is finally obtained depends on the initial condition.

6. Summary and conclusion

We analyzed a numerical scheme based on a Fourier spectral method for an epitaxial growth model without slope selection. The main idea of the method was extracted from the decomposition of the free energy associated with the model into the difference of two convex functions. The numerical algorithm stated treats the fourth order linear term implicitly and handles the nonlinear term explicitly. We theoretically and numerically demonstrated the convergence of our model to the critical points of the free energy using a Lojasiewicz-Simon inequality. Numerical simulations accommodate the theoretical results. Critical points which correspond to the stationary solution of the model without slope selection are computed by means of long time simulations of the coarsening process until convergence.

Acknowledgements

The authors are thankful to the two anonymous referees who helped improve the quality of the paper.

References

[1] W. Chen, S. Conde, C. Wang, X. Wang, and S. M. Wise. A linear energy stable scheme for a thin film model without slope selection. J. Sci. Comput., 52 (2012) 546–562.

[2] W. Chen, C. Wang, X. Wang, and S. M. Wise. A linear iteration algorithm for a second-order energy stable scheme for a thin film model without slope selection. J. Sci. Comput., 59 (2014) 574–601.

[3] R. Du, Z.-z. Sun, and G.-h. Gao. A second-order linearized three-level backward Euler scheme for a class of nonlinear expitaxial growth model. Int. J. Comput. Math., 92 (2015) 2290–2309.

[4] L. Golubović. Interfacial coarsening in epitaxial growth models without slope selection. Phys. Rev. Lett., 78 (Jan 1997) 90–93.
[5] M. Grasselli, G. Mola, and A. Yagi. On the longtime behavior of solutions to a model for epitaxial growth. Osaka J. Math., 48 (2011) 987–1004.
[6] M. Guedda and H. Trojette. Coarsening in an interfacial equation without slope selection revisited: Analytical results. Phys. Lett. A, 374 (2010) 4308–4311.
[7] A. Haraux and M. A. Jendoubi. *The convergence problem for dissipative autonomous systems*. SpringerBriefs in Mathematics. Springer, Cham; BCAM Basque Center for Applied Mathematics, Bilbao, 2015.
[8] M. Johnson, C. Orme, A. Hunt, D. Graff, J. Sudijono, L. Sander, and B. Orr. Stable and unstable growth in molecular beam epitaxy. Phys. Rev. Lett., 72 (1994) 116–119.
[9] L. Ju, X. Li, Z. Qiao, and H. Zhang. Energy stability and error estimates of exponential time differencing schemes for the epitaxial growth model without slope selection. Math. Comp., 87 (2018) 1859–1885.
[10] O. Kavian. *Introduction à la théorie des points critiques et applications aux problèmes elliptiques*, volume 13 of *Mathématiques & Applications (Berlin)*. Springer-Verlag, Paris, 1993.
[11] H. G. Lee, J. Shin, and J.-Y. Lee. A second-order operator splitting Fourier spectral method for models of epitaxial thin film growth. J. Sci. Comput., 71 (2017) 1303–1318.
[12] B. Li and J.-G. Liu. Thin film epitaxy with or without slope selection. European J. Appl. Math., 14 (2003) 713–743.
[13] B. Li and J.-G. Liu. Epitaxial growth without slope selection: energetics, coarsening, and dynamic scaling. Int. J. Nonlinear Sci, 14 (2004) 429–451.
[14] S. Łojasiewicz. Ensembles semi-analytiques. *Lectures Notes I.H.E.S. (Bures-sur-Yvette)*, 1965.
[15] B. Merlet and M. Pierre. Convergence to equilibrium for the backward Euler scheme and applications. Commun. Pure Appl. Anal., 9 (2010) 685–702.
[16] M. Pierre and P. Rogeon. Convergence to equilibrium for a time semi-discrete damped wave equation. J. Appl. Anal. Comput., 6 (2016) 1041–1048.
[17] P. Politi and J. Villain. Ehrlich-Schwoebel instability in molecular-beam epitaxy: A minimal model. Phys. Rev. B, 54 (1996) 5114.
[18] Z. Qiao, Z.-Z. Sun, and Z. Zhang. Stability and convergence of second-order schemes for the nonlinear epitaxial growth model without slope selection. Math. Comp., 84 (2015) 653–674.
[19] R. L. Schwoebel. Step motion on crystal surfaces. II. J. Appl. Phys, 40 (1969) 614–618.
[20] A. Yassine, N. Alaa, and A. Elhilali Alaoui. Convergence of Toland's critical points for sequences of DC functions and application to the resolution of semilinear elliptic problems. Control Cybern., 30 (2001) 405–417.

LAMAI Laboratory, Faculty of Science and Technology, Cadi Ayyad University, Marrakesh, Morocco.
E-mail: `hamza.khalfi@edu.uca.ma`

Laboratoire de Mathématiques et Applications, Université de Poitiers, CNRS, F-86962 Chasseneuil, France.
E-mail: `morgan.pierre@math.univ-poitiers.fr`

LAMAI Laboratory, Faculty of Science and Technology, Cadi Ayyad University, Marrakesh, Morocco.
E-mail: `n.alaa@uca.ac.ma`

LAMFA Laboratory, CNRS UMR 7352, Picardie Jules Verne University, Amiens, France.
E-mail: `mohamed.guedda@u-picardie.fr`